The survival of fetal and bone marrow monocyte-derived alveolar macrophages is promoted by CD44 and its interaction with hyaluronan

Y Dong[1], GFT Poon[1], AA Arif[1], SSM Lee-Sayer[1], M Dosanjh[1] and P Johnson[1]

Alveolar macrophages maintain lung homeostasis by performing important roles in immunosurveillance and lung surfactant catabolism. They express high levels of CD44 and are one of the few macrophage populations that constitutively bind hyaluronan, a ligand for CD44 and component of pericellular and extracellular matrices. Using adoptive transfer experiments and a mouse model of inflammation, we found that alveolar macrophages are initially depleted after an inflammatory insult then rapidly self-renew and return to original numbers after the resolution phase. Monocytes recruited to an inflamed lung differentiate and contribute to the alveolar macrophage pool, but this occurs over a much slower time frame than alveolar macrophage self-renewal. CD44 expression on both fetal and bone marrow-derived alveolar macrophages promoted their survival and provided a competitive advantage over CD44-deficient alveolar macrophages at homeostasis and after inflammation. CD44-mediated hyaluronan binding was induced by the alveolar environment, and this interaction promoted alveolar macrophage survival both *ex vivo* and *in vivo*. Without CD44, alveolar macrophages lacked a hyaluronan coat, were more susceptible to death, and were present at lower numbers in the alveolar space. This demonstrates a new role for CD44 and hyaluronan in promoting alveolar macrophage survival.

INTRODUCTION

The airways are primary entry sites for pathogens and airborne particles[1,2] where alveolar macrophages (AMΦ) are a first line of defense to phagocytose pathogens, particulates, and cell debris.[1–3] Shortly after birth, colony stimulating factor-2 (CSF-2 or granulocyte-macrophage-CSF) drives the differentiation of fetal monocytes into long-lived AMΦ capable of self-renewal.[4–7] Their self-renewal is sufficient to maintain the AMΦ population at homeostasis and does not require replenishment from bone marrow (BM)-derived monocytes.[3,6,7] However, BM-derived cells are capable of developing into AMΦ, as after AMΦ ablation by irradiation, subsequent BM reconstitution leads to BM-derived AMΦ in adult mice.[8] Yolk sac macrophages, fetal liver, and adult monocytes can colonize the lungs of Csf2rb$^{-/-}$ mice and develop into functional AMΦ,[9] showing that progenitors of different origins can differentiate into AMΦ, raising the possibility that it is the alveolar environment, not the origin of the progenitor, that determines their differentiation into AMΦ.[10] In acute inflammation, the numbers of AMΦ are reduced and then restored after inflammation is resolved. In influenza infection, the recovery of AMΦ was attributed to AMΦ self-renewal,[7] whereas 2 months after acute lipopolysaccharide (LPS)-induced inflammation, the majority of AMΦ were shown to be BM derived.[11] Thus, in adult mice, the extent to which monocytes contribute to AMΦ renewal after inflammation[10] is not clear, nor are the factors that regulate monocyte differentiation and AMΦ renewal after inflammation. Such information would considerably aid the understanding of the AMΦ renewal process that could be crucial for the resolution of inflammation and return to homeostasis.

At homeostasis, AMΦ are thought to exist in a somewhat immunosuppressive environment where they phagocytose pathogens without alerting other innate immune cells.[3] If they cannot clear the infection, they initiate innate immune responses: for example, in response to *Streptococcus*

[1]Department of Microbiology and Immunology, University of British Columbia, Vancouver, British Columbia, Canada. Correspondence: P Johnson (pauline@mail.ubc.ca)

Received 11 February 2017; revised 7 August 2017; accepted 16 August 2017; published online 25 October 2017. doi:10.1038/mi.2017.83

pneumoniae[12] and respiratory syncytial virus.[13] However, AMΦ depletion can also exacerbate pulmonary inflammatory responses,[14,15] suggesting AMΦ have an anti-inflammatory role, but the loss of AMΦ could also lead to greater damage to other cells that further stimulates the immune response. Murine AMΦ are characterized by the expression of CD11c, Siglec F[3], as well as their expression of CD44 and the ability to constitutively bind hyaluronan (HA).[16] CD44 is responsible for the binding and uptake of HA in AMΦ *in vitro* and during lung development after birth.[17,18] In bleomycin-induced lung inflammation, $CD44^{-/-}$ mice have increased HA accumulation, a buildup of apoptotic neutrophils, and the mice die from unremitting inflammation.[19] This phenotype is partially rescued if the mice are reconstituted with $CD44^{+/+}$ BM,[19,20] implicating a key role for CD44 in HA clearance and resolution of lung inflammation. CD44 also contributes to neutrophil recruitment to inflammatory sites,[21] raising the possibility that CD44 may also contribute to monocyte recruitment to the lungs. Given the constitutive HA binding ability of AMΦ, we sought to evaluate the significance of CD44 and HA binding in AMΦ homeostasis and renewal under normal and inflammatory conditions.

RESULTS

$CD44^{-/-}$ mice have reduced numbers of AMΦ and $CD44^{-/-}$ AMΦ are at a competitive disadvantage under both homeostatic and inflammatory conditions

To determine the significance of constitutive HA binding and CD44 expression by AMΦ in the alveolar space, we compared *bona fide* fetal monocyte-derived AMΦ from $CD44^{+/+}$ and $CD44^{-/-}$ mice. The number of AMΦ isolated from the bronchoalveolar lavage (BAL) of $CD44^{-/-}$ mice was significantly lower compared with $CD44^{+/+}$ mice (**Figure 1a**). A reduction was also observed in AMΦ isolated from the lung where equivalent numbers of lung cells were isolated from $CD44^{+/+}$ and $CD44^{-/-}$ mice, ruling out differences in location or total cell numbers in the lungs between the mice (**Figure 1b**). No gross differences were observed in the expression of Siglec F, CD11c, or CD11b between the $CD44^{+/+}$ and $CD44^{-/-}$ AMΦ (**Figure 1a,b**). This suggested an intrinsic defect in the $CD44^{-/-}$ AMΦ, although the alveolar environment can also have a strong influence on AM survival and maturation.[4–6,22] To distinguish between these possibilities, AMΦ were isolated from $CD45.2^{+}$ $CD44^{+/+}$ and $CD44^{-/-}$ mice and instilled into the alveolar space of $CD44^{+/+}$ $CD45.1^{+}$ mice in a 1:1 ratio (**Figure 1c**). After 24 h, there was still a 1:1 ratio of donor $CD44^{+/+}$ and $CD44^{-/-}$ AMΦ in the BAL, demonstrating no advantage of CD44 on the initial engraftment (**Figure 1d,g**). However, by day 8 after instillation, there was >2:1 ratio of donor $CD44^{+/+}$ AMΦ over $CD44^{-/-}$ (**Figure 1e,h**), indicating a competitive advantage of $CD44^{+/+}$ AMΦ. As the reduced percentage of $CD44^{-/-}$ AMΦ was observed in a CD44-sufficient lung environment, this supports an intrinsic defect in these cells. To determine whether instillation of the donor AMΦ into an inflammatory lung environment would affect the outcome, we instilled LPS 24 h after the instillation of the 1:1 ratio of donor AMΦ. Analysis of the cells at day 7 after LPS (day 8 after AMΦ instillation) revealed a similar 2:1 ratio (**Figure 1f,h**), indicating no further advantage. It was noted that there were more $CD45.2^{-}$ $CD11c^{+}$ host cells at day 7 after LPS treatment compared with untreated (**Figure 1i**). In a different experiment, a comparison of the number of instilled donor GFP^{+} $CD44^{+/+}$ AMΦ before and after LPS-induced inflammation showed a threefold increase of AMΦ on day 7 after LPS relative to days 0 and 1 (**Figure 1j**), indicating that AMΦ had proliferated in response to LPS-induced inflammation. Thus, $CD44^{-/-}$ AMΦ have an intrinsic defect that compromised their ability to generate normal numbers of AMΦ in the alveolar space at homeostasis and decreased their ability to compete with $CD44^{+/+}$ AMΦ under both homeostatic and inflammatory conditions.

CD44 provides an advantage to monocyte-derived AMΦ

To determine whether this CD44 advantage also extends to BM monocyte-derived AMΦ, we performed a competitive BM reconstitution using $CD44^{-/-}$ and $CD44^{+/+}$ BM cells into a lethally irradiated CD44-sufficient host. Unlike at homeostasis, this creates an empty niche in the alveolar space, allowing full reconstitution of AMΦ from BM monocytes.[8] The donor BM cells were distinguishable by CD44 expression and by CD45.1 and CD45.2 allogeneic markers: $CD44^{-/-}$ BM was $CD45.2^{+}$ and $CD44^{+/+}$ BM was $CD45.1^{+}$ $CD45.2^{+}$. BM cells were isolated, mixed in a 1:1 ratio, and 8 million cells were injected intravenously (IV) into lethally irradiated $CD45.1^{+}$ mice (**Figure 2a**). Seven weeks elapsed to allow for BM reconstitution and then the percentage chimerism was determined in the lung. Monocytes ($Ly6C^{high}$ $CD11c^{-}$), neutrophils ($Ly6G^{+}$), and eosinophils ($Ly6C^{low}$ side scatter $(SSC)^{high}$) all showed equal chimerism of ~1:1 (**Figure 2b,c**). However, AMΦ ($CD11c^{+}$ FSC^{high}) showed a 3:1 ratio of $CD44^{+/+}/CD44^{-/-}$ cells indicating a significant advantage for $CD44^{+/+}$ AMΦ in the lung (**Figure 2b,c**). Isolation of $CD11c^{+}$ AMΦ from the BAL, where they constitute the majority of cells, further demonstrated a 3:1 ratio and a distinct advantage for $CD44^{+/+}$ AMΦ (**Figure 2b,c**). Although CD44 is expressed on neutrophils, eosinophils, and $Ly6C^{high}$ monocytes, it does not confer a competitive advantage after BM reconstitution in these cells, whereas it does for AMΦ.

LPS-induced lung inflammation causes a transient loss of AMΦ and differentiated monocytes gain HA binding

We next wanted to investigate whether the CD44 advantage of monocyte-derived AMΦ occurred in a more physiological setting. Furthermore, it was of interest to determine to what extent self-renewal or monocyte recruitment contributes to the AMΦ population after inflammation. In order to study this, we first established a suitable acute lung inflammation mouse model using LPS. The course of LPS-induced inflammation was monitored over time by weight loss (**Figure 3a**) and the total number of leukocytes present in the BAL (**Figure 3b**) that indicated the peak of inflammation occurred around day 3 and was resolved by day 14. Flow cytometry of the BAL cells,

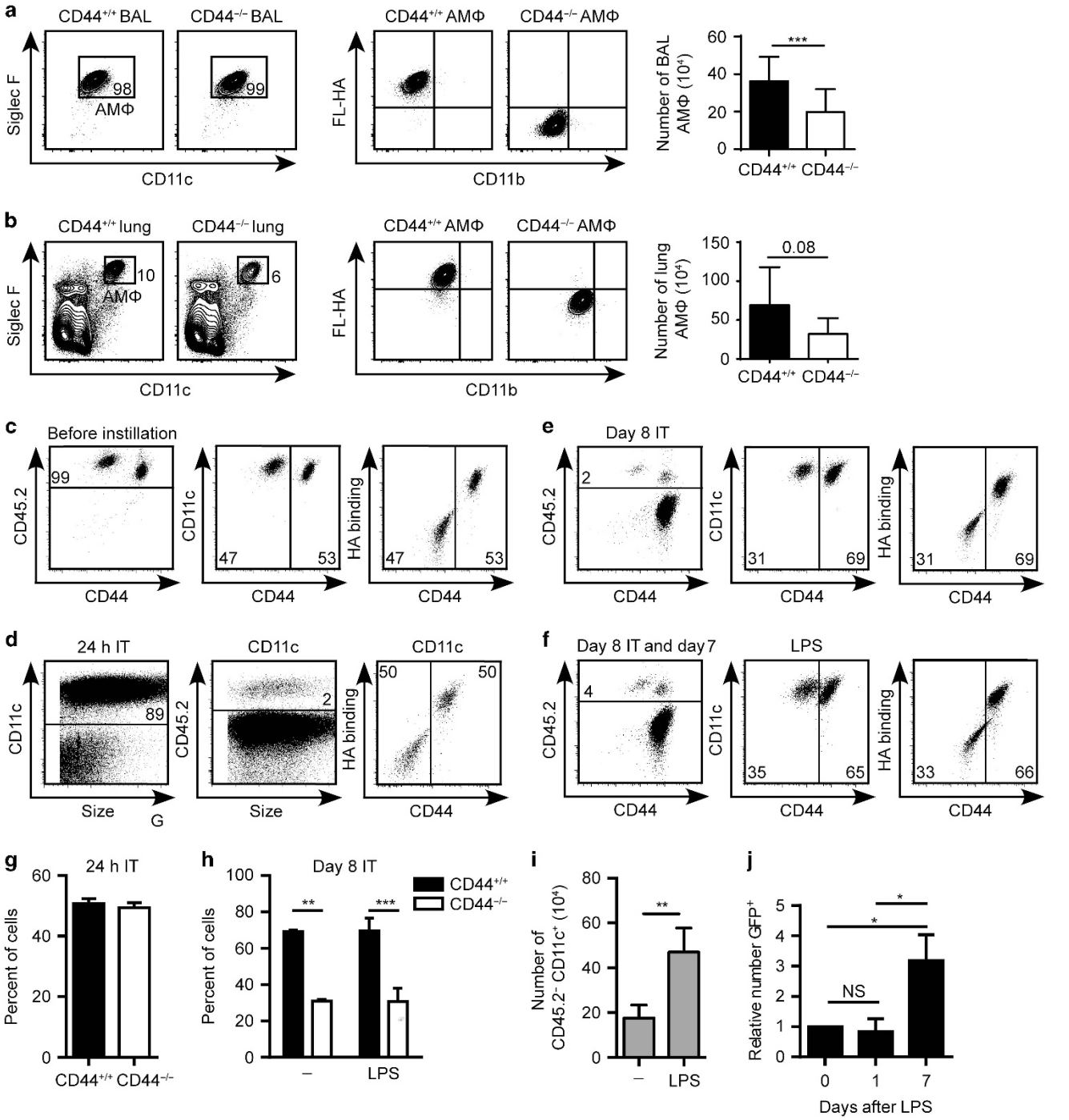

Figure 1 CD44 deficiency reduces alveolar macrophage (AMΦ) numbers. (**a**) Representative flow cytometry plots and graph of 40 mice comparing the phenotype and number, respectively, of AMΦ isolated from the bronchoalveolar lavage (BAL) of CD44$^{+/+}$ and CD44$^{-/-}$ mice. (**b**) Representative flow cytometry plots and graph of 16 mice showing the phenotype and number, respectively, of AMΦ from the lungs of CD44$^{+/+}$ and CD44$^{-/-}$ mice after BAL removal. (**c**) Flow cytometric analysis of 3×10^5 CD45.2$^+$ donor CD44$^{+/+}$ and CD44$^{-/-}$ AMΦ mixed in a 1:1 ratio before intratracheal (IT) instillation into CD45.1$^+$CD45.2$^-$ host mice. (**d**) Proportion of donor CD44$^{+/+}$ and CD44$^{-/-}$ AMΦ in the BAL 24 h after instillation. (**e**) Proportion of donor CD44$^{+/+}$ and CD44$^{-/-}$ AMΦ in the BAL after 8 days. (**f**) Proportion of donor CD44$^{+/+}$ and CD44$^{-/-}$ AMΦ in the BAL after 8 days, treated with lipopolysaccharide (LPS) via IT instillation 24 h after AMΦ transfer. (**g**) Percent of donor CD44$^{+/+}$ and CD44$^{-/-}$ AMΦ in the BAL 24 h after instillation. (**h**) Percent of donor CD44$^{+/+}$ and CD44$^{-/-}$ AMΦ after 7 days with or without LPS treatment. (**i**) Total number of host CD45.2$^-$ CD11c$^+$ cells in the BAL after 7 days of with or without LPS treatment. (**j**) GFP$^+$ CD44$^+$ AMΦ were instilled into the lungs for 24 h (day 0) and then LPS was instilled into the lungs and the number GFP$^+$ AMΦ counted at days 1 and 7 after LPS. Relative cell numbers compared with day 0 are shown. In **c**–**j**, data show an average of two experiments ± s.d., each with three to five mice. Significance indicated as $^*P<0.05$, $^{**}P<0.01$, $^{***}P<0.001$, nonpaired (**a**, **b**, **i**, **j**) and paired Student's *t*-test (**g**, **h**), NS, not significant.

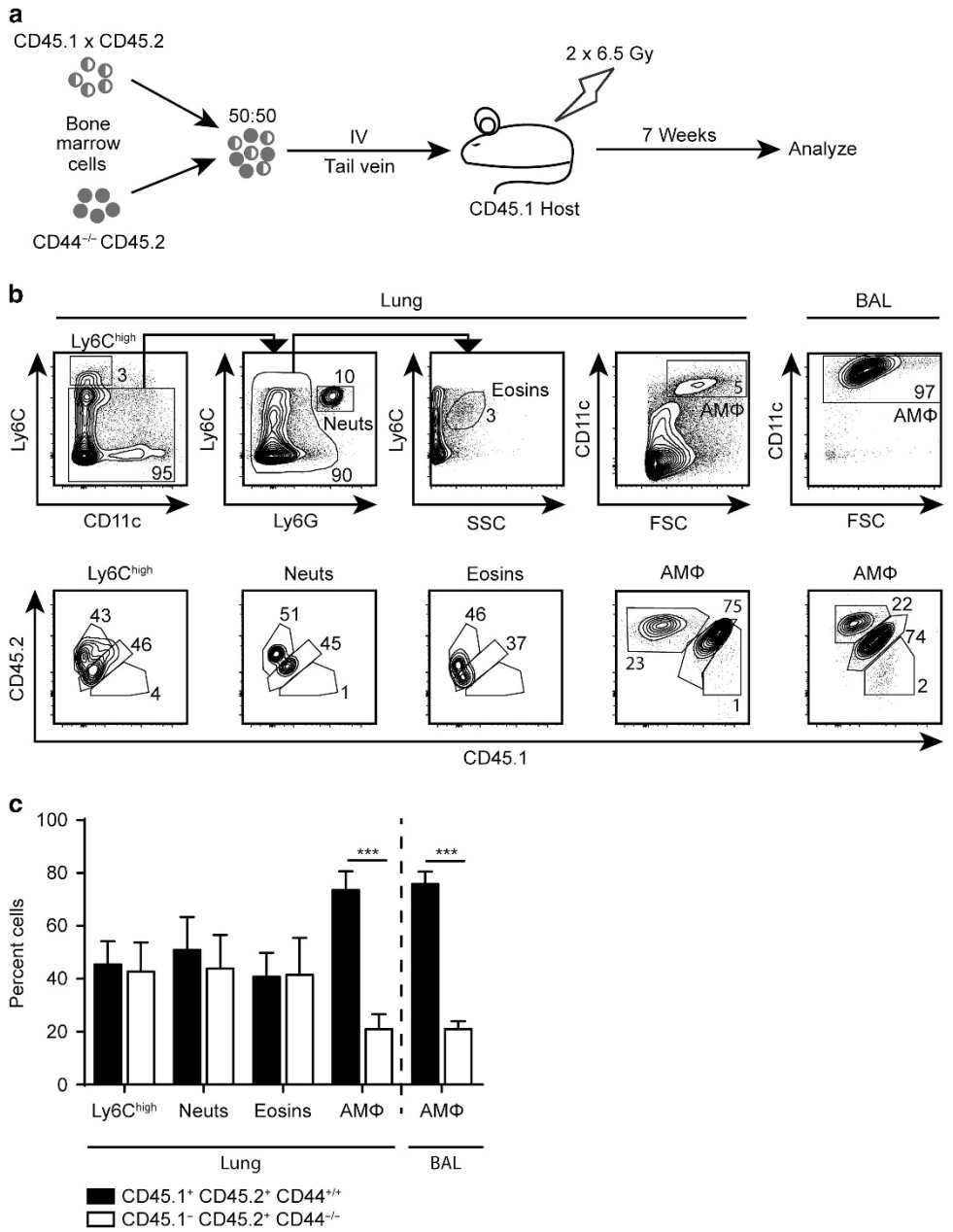

Figure 2 CD44 deficiency impairs alveolar macrophage (AMΦ) repopulation following lethal irradiation. (**a**) Schematic showing bone marrow (BM) reconstitution of lethally irradiated CD45.1$^+$ host mice with 8 million BM cells from CD45.1$^+$ CD45.2$^+$ CD44$^{+/+}$ and CD45.1$^-$ CD45.2$^+$ CD44$^{-/-}$ mice in a 1:1 ratio, analyzed after 7 weeks. (**b**) Representative flow cytometry plots showing the identification and proportions of CD44$^{+/+}$ and CD44$^{-/-}$ neutrophils, eosinophils, Ly6C^{high} cells, AMΦ in the lung, and AMΦ in the bronchoalveolar lavage (BAL) 7 weeks after reconstitution. (**c**) Graph showing the proportion of CD44$^{+/+}$ and CD44$^{-/-}$ cells in the different myeloid populations in the lung and BAL after reconstitution. Data show an average of two experiments ± s.d., each with three to five mice. Significance indicated as ***$P<0.001$, paired Student's *t*-test.

identifying the AMΦ as well as incoming monocytes and neutrophils, revealed a significant depletion of CD11c$^+$ SiglecF$^+$ AMΦ occurring early in the response at day 1, together with an influx of CD11b$^+$ Ly6G^{high} neutrophils, followed by an influx of CD11b$^+$ Ly6C^{high} monocytes that peaked at day 3 after stimulation (**Figure 3c–f**). Despite their initial loss, AMΦ quickly repopulated and expanded beyond preinflammatory values by day 7 (**Figure 3d**). In addition, by day 7, CD11b$^+$ Ly6C^{high} monocytes were replaced with CD11b$^+$ Ly6C$^-$ CD11c$^{+/-}$ cells (**Figure 3c**). Most of these became CD11c$^+$, gained Siglec F, and lost CD11b expression by day 14, suggesting further differentiation. Interestingly, as the monocytes differentiated, they also gained HA binding, another hallmark of AMΦ. By day 30, these cells were either absent or indistinguishable from resident AMΦ (CD11c$^+$, Siglec F$^+$, HA binding) (**Figure 3c,e**). Overall, this raises the possibility that the transiently depleted AMΦ are capable of rapid self-renewal, whereas the recruited monocytes may

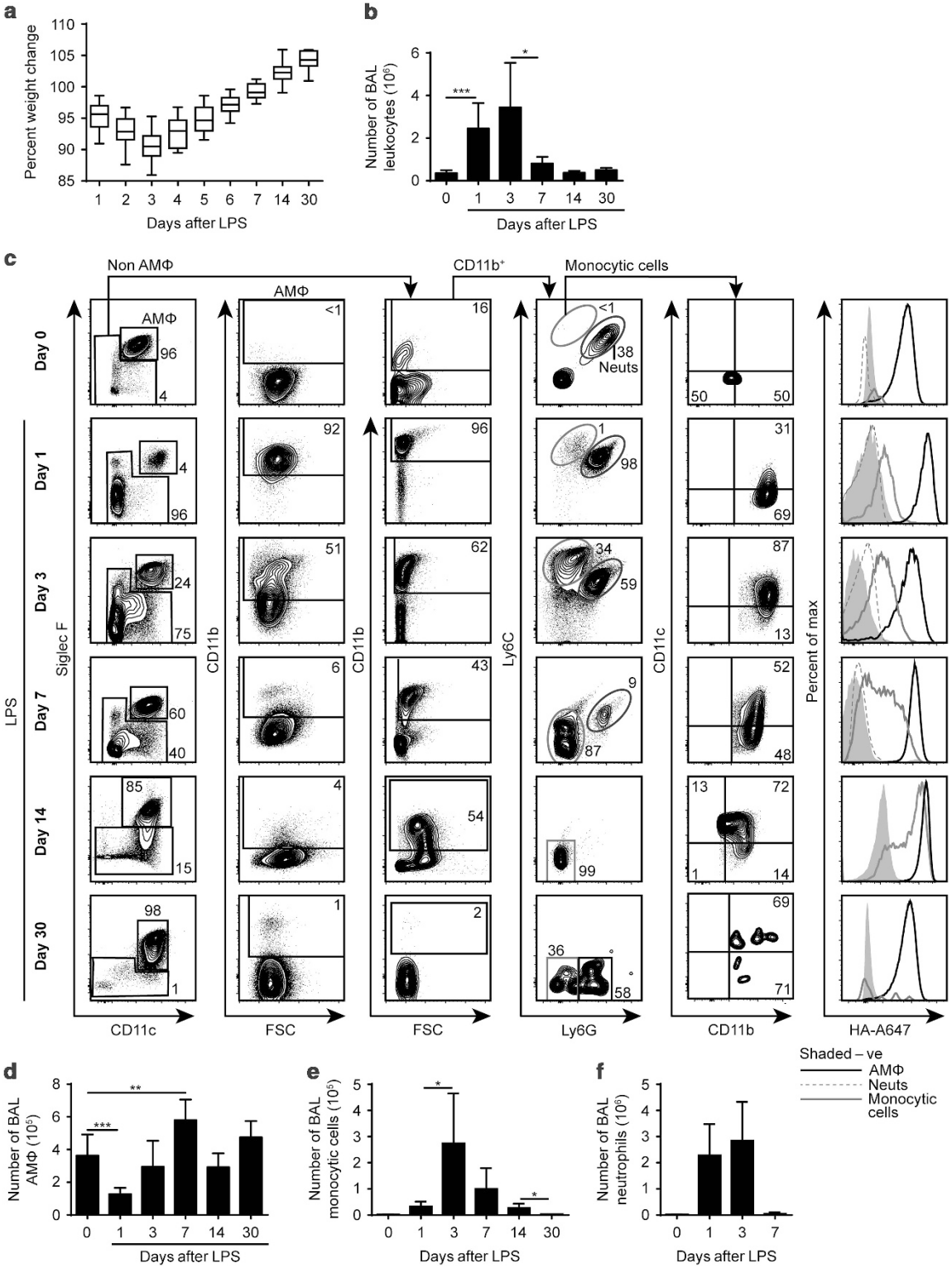

Figure 3 Characterization of inflammatory cells in the bronchoalveolar lavage (BAL) during lipopolysaccharide (LPS)-induced lung inflammation. (**a**) Change in body weight of mice after treatment with 25 μg of LPS via intratracheal (IT) instillation. (**b**) Number of total leukocytes in the BAL during LPS-induced lung inflammation. (**c**) Representative flow cytometry plots showing cell populations and their phenotype in the BAL at steady state (day 0) and during LPS-induced lung inflammation. Histograms show hyaluronan (HA) binding of the different populations. (**d**) Number of alveolar macrophages (AMΦ), gated as in **c**, in the BAL at steady state and throughout the response to LPS. (**e**) Number of infiltrated monocytes, gated as in (**c**), in the BAL in response to LPS. (**f**) Number of neutrophils, gated as in **c**, in the BAL during LPS-induced inflammation. Flow cytometry plots were first gated by size, singlets, and live/dead stain. Data show an average of two experiments ± s.d., each with three to five mice. Significance indicated as $^{*}P<0.05$, $^{**}P<0.01$, $^{***}P<0.001$, nonpaired Student's *t*-test.

undergo a slower differentiation process to eventually become AMΦ 1 month after recruitment.

GFP$^+$ monocytes mature into AMΦ 30 days after the inflammatory stimulus

To determine whether the recruited monocytes disappear over time or differentiate into AMΦ, we followed the fate of adoptively transferred GFP$^+$ monocytes. Steady-state AMΦ were CD11b$^-$ Ly6C$^-$ Ly6G$^-$ CD11c$^+$ Siglec F$^+$ and HA binding (**Figure 4a**). GFP$^+$ monocytes (CD11b$^+$ Ly6C^{high} Ly6G$^-$ CD11c$^-$ Siglec F$^-$ and non-HA binding) were isolated from the BM of GFP$^+$ mice with ~95% purity (**Figure 4b**) and 0.5–1 × 10^6 monocytes were injected IV 4 h after intratracheal (IT) instillation of LPS. Perfused lung tissue and the BAL were harvested over time to analyze the fate of the recruited GFP$^+$ monocytes. GFP$^+$ cells were recruited to the BAL of inflamed mice on day 1 and maintained their monocyte phenotype: CD11b$^+$ Ly6C^{high} Ly6G$^-$ CD11c$^-$ Siglec F$^-$ and non-HA binding (**Figure 4b**). By day 3, monocytes were losing Ly6C expression and by day 7 this had largely disappeared. Cells started to gain CD11c at day 7 and by day 14 were mostly CD11c$^+$ and CD11b$^-$, and many had gained the ability to bind HA and express Siglec F (**Figure 4b**). By day 30, the GFP$^+$ cells were indistinguishable from the characteristic phenotype of AMΦ: CD11b$^-$ CD11c$^+$ Siglec F$^+$ and HA binding. These phenotypic changes in the green fluorescent protein (GFP) monocytes mirrored those of the host monocytes observed in **Figure 3**. In addition, the number of GFP$^+$ cells in the BAL peaked at day 3, as did host monocytes, then the number of GFP$^+$ cells in the BAL decreased to a minimum at day 14, and then increased at day 30 (**Figure 4c**), suggesting that either the differentiated monocytes proliferated or entered the alveolar space from the lung tissue. The reduction in GFP$^+$ cells in the lung between days 14 and 30 (**Figure 4c**) supports the latter possibility at day 30; however, detection of a small percentage of Ki67$^+$ GFP$^+$ cells at day 45 also supports cell proliferation that occurred at a comparable rate to the host AMΦ (**Figure 4d**). Furthermore, these GFP$^+$ cells at day 45 were phenotypically indistinguishable from host AMΦ, by the expression levels of CD11c, Siglec F, CD11b, HA binding, SIRPα, CD206, and F4/80 (**Figure 4e**).

CD44 exerts an advantage in monocyte-derived AMΦ after inflammation

Having identified that AMΦ can repopulate a few days after depletion by an inflammatory insult such as LPS, and that recruited monocytes can differentiate into a phenotypically identical AMΦ by day 30, we can now examine the effect of CD44 on AMΦ repopulation by self-renewal and from monocytes. To determine when CD44 influenced monocyte-derived AMΦ repopulation after inflammation, we repeated the above experiment using a 1:1 ratio of CD45.2$^+$ CD44$^{+/+}$ and CD44$^{-/-}$ monocytes purified from the BM of the respective mice injected IV into CD45.1$^+$ mice, 4 h after IT LPS injection (**Figure 5a,b**). Analysis of the BAL cells 14 days after induction of inflammation revealed the percent and phenotype of CD44$^{+/+}$ or CD44$^{-/-}$ cells within the CD45.2$^+$ donor cells population were similar (**Figure 5c,e**), indicating no selective advantage of CD44 at this stage of differentiation in the BAL when differentiating monocytes begin to gain CD11c, Siglec F, and HA binding. However, at day 30 when monocytes fully adopted the AMΦ phenotype, there was a similar 3:1 advantage of CD44$^{+/+}$ cells over CD44$^{-/-}$ cells (**Figure 5d,f**). This demonstrated that CD44 did not affect the recruitment of monocytes. Instead, the competitive CD44 advantage materializes by day 30 when monocytes have differentiated into AMΦ and gained HA binding.

The alveolar environment induces HA binding

The alveolar environment and CSF-2 are important for the development and maturation of fetal monocyte-derived AMΦ.[4–6] To determine whether the alveolar environment can induce HA binding in macrophages, F4/80$^+$ macrophages were isolated from the peritoneal lavage. Over 85% of the cells were F4/80^{high} MHCII^{low} macrophages and ~10% F4/80^{low} MHCII^{high} (**Figure 6a**), consistent with a majority of tissue-resident peritoneal macrophages and a minority of small peritoneal macrophages, as described in ref.[23] These peritoneal macrophages (PMΦ) were CD11c$^-$ CD11b$^+$ and non-HA binding (**Figure 6b**), and phenotypically distinct from AMΦ. GFP$^+$ PMΦ were instilled into the lungs of wild-type, non-irradiated mice, and isolated from the BAL 2 weeks later where they had gained similar levels of CD11c and HA binding as the resident AMΦ, but remained CD11b$^+$ (**Figure 6c**). This demonstrated that the alveolar environment induces HA binding. CSF-2 may induce CD44 to bind HA in the alveolar space, as CSF-2- but not CSF-1-derived BMDMs (BM-derived macrophages) bound HA.[16,24] Furthermore, CSF-2-derived BMDMs have several phenotypic and functional similarities to AMΦ.[16] To investigate this, CSF-1-derived BMDMs were cultured with CSF-2 for 48 h and this partially upregulated their HA binding ability and CD11c expression (**Figure 6d**). To test whether CSF-2 also induced PMΦ to bind HA, PMΦ were cultured with CSF-2 for 7 days *in vitro*. This did not induce HA binding in PMΦ, neither did the peroxisome proliferator-activated receptor-γ (PPARγ) agonist rosiglitazone (ROZ),[25] but together they significantly induced HA binding in the PMΦ (**Figure 6e**).

CD44 and HA binding promote AMΦ survival

To determine how CD44 was providing an advantage for AMΦ, we isolated CD44$^{-/-}$ and CD44$^{+/+}$ AMΦ from the BAL, and labeled these *ex vivo* AMΦ with Ki67 antibody, a marker of cell proliferation. The percentage of Ki67$^+$ AMΦ was not significantly different (**Figure 7a**), suggesting no difference in cell cycling or proliferation rate at the steady state. However, when *ex vivo* AMΦ were labeled with 4',6-diamidino-2-phenylindole (DAPI) and Annexin V, CD44$^{-/-}$ AMΦ showed significantly more apoptotic and dead cells than CD44$^{+/+}$ AMΦ (**Figure 7b,c**). Less viable *ex vivo* CD44$^{-/-}$ AMΦ were also observed after equal numbers were cultured for 24 h (**Figure 7c**). This showed that CD44 was providing a survival advantage for AMΦ, possibly by providing a survival signal to AMΦ. Given the distinct constitutive HA binding

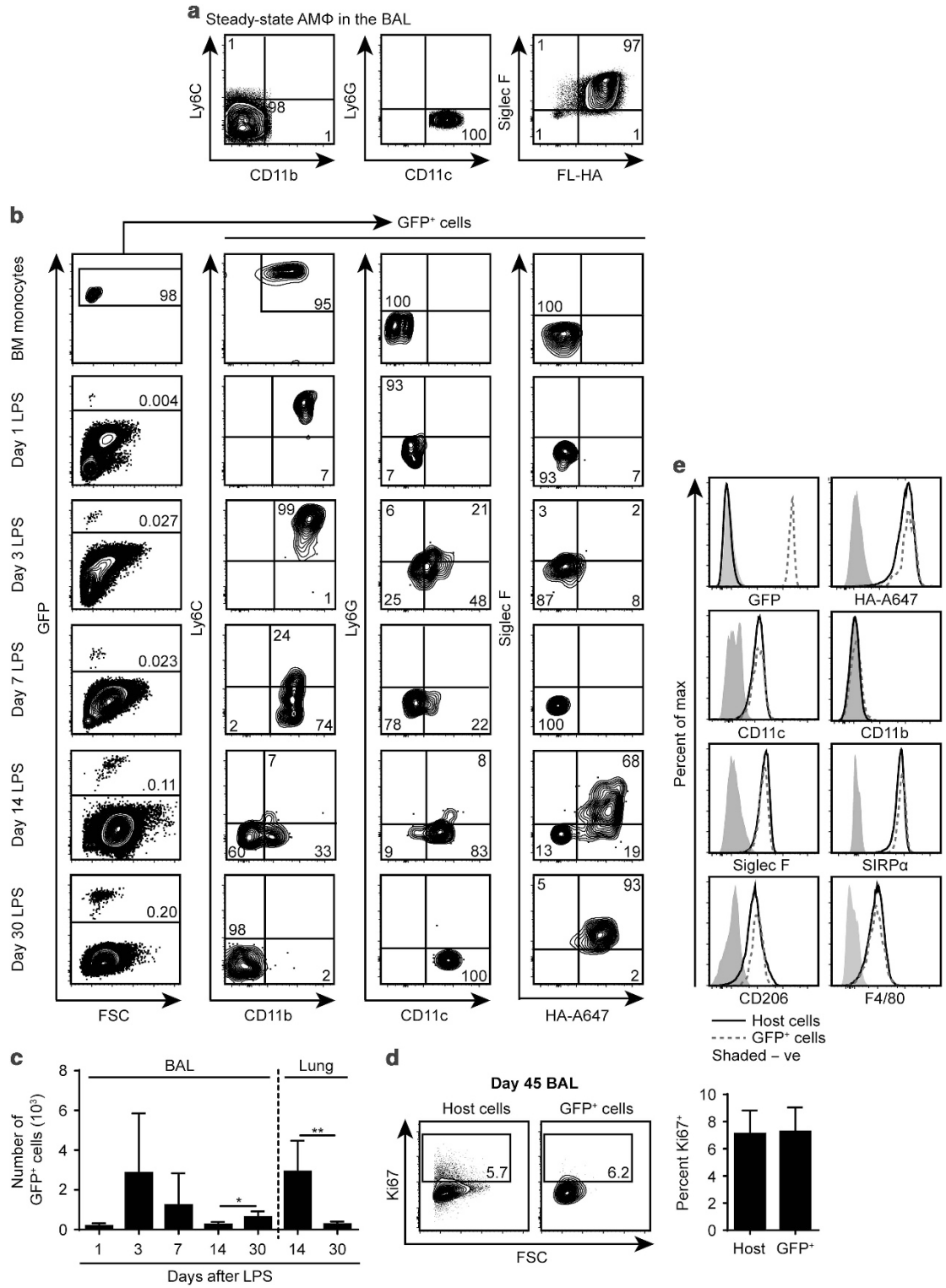

Figure 4 Adoptively transferred bone marrow (BM) monocytes give rise to alveolar macrophages (AMΦ) following lipopolysaccharide (LPS)-induced lung inflammation. (**a**) Representative flow cytometry plots showing the expression levels of Ly6C, CD11b, Ly6G, CD11c, Siglec F, and fluorescein-conjugated HA (FL-HA) binding by AMΦ at steady state. (**b**) Representative flow cytometry plots showing the phenotype of GFP$^+$ monocytes isolated from the BM and the phenotypic changes in the bronchoalveolar lavage (BAL) after they were adoptively transferred intravenously (IV) into mice treated with 25 μg LPS intratracheally (IT) 4 h earlier. (**c**) Number of GFP$^+$ donor cells in the host BAL and lung throughout the LPS response. (**d**) Representative flow cytometry plots and graph comparing Ki67 expression in GFP$^+$ donor cells and host AMΦ. (**e**) Histograms representative of 12 mice from two experiments comparing the phenotype of GFP$^+$ donor cells and host AMΦ 45 days after LPS treatment. Data show an average from two experiments ± s.d., each with three to five mice. Significance indicated as $^*P<0.05$, $^{**}P<0.01$, nonpaired Student's *t*-test.

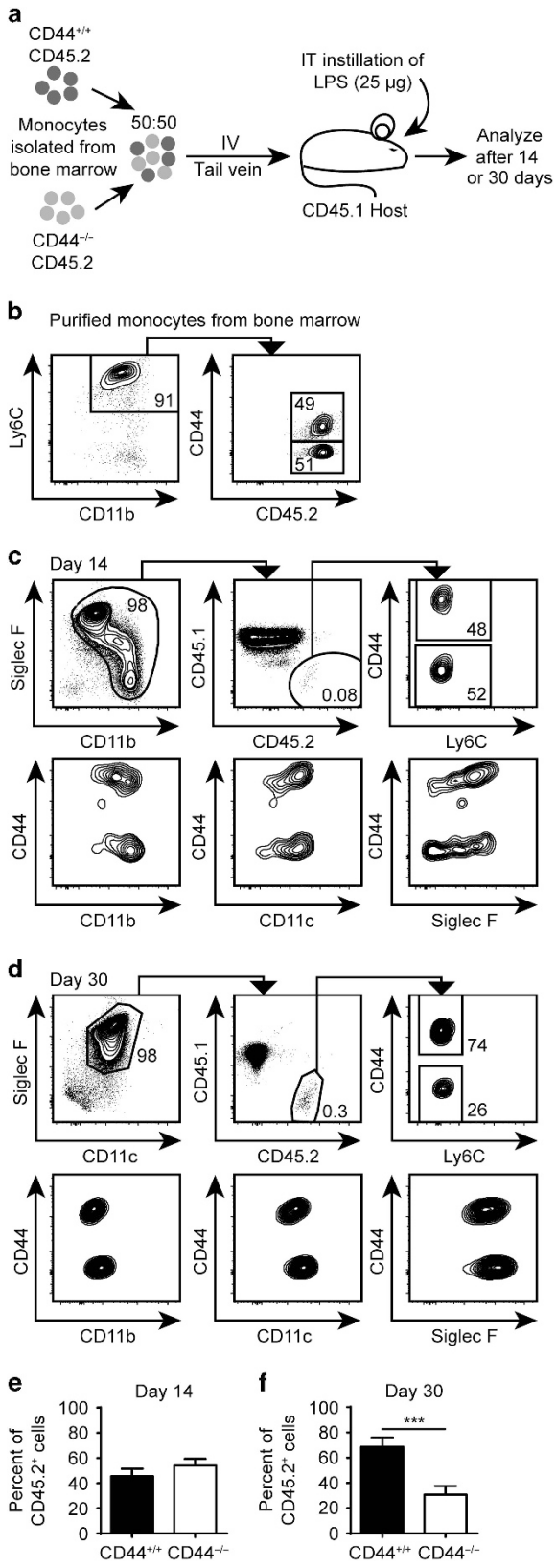

ability of CD44 on AMΦ, we investigated whether CD44 was binding to HA in the alveolar space. HA was detected by HA binding protein (HABP) that revealed intense staining around the bronchioles and identified CD11c$^+$ Siglec F$^+$ AMΦ as the major cells in the BAL that bound HA *in vivo*. In contrast, CD44$^{-/-}$ AMΦ were poorly labeled by HABP, indicating significantly less surface HA (**Figure 7d,e**). This suggested that CD44$^{+/+}$ AMΦ, but not CD44$^{-/-}$ AMΦ, were decorated with a HA coat. Further analysis by flow cytometry on *ex vivo* AMΦ from the BAL confirmed that CD44$^{+/+}$ AMΦ were decorated with surface HA to a much greater extent than CD44$^{-/-}$ AMΦ (**Figure 7f**), suggesting the cell surface HA was bound to CD44.

Incubation of CD44$^{+/+}$ AMΦ with bovine hyaluronidase significantly reduced HABP labeling, indicating HABP binding was specific for surface HA (**Figure 8a,b**). To determine the significance of this HA binding and its possible role in AMΦ survival, *ex vivo* CD44$^{+/+}$ and CD44$^{-/-}$ AMΦ were incubated in phosphate-buffered saline (PBS), with or without bovine hyaluronidase or the HA blocking CD44 monoclonal antibody (mAb), KM81, for 1 h and then labeled with DAPI and Annexin V. Both HA removal and KM81 addition decreased the viability of CD44$^{+/+}$ AMΦ to the levels observed with the CD44$^{-/-}$ AMΦ, and these treatments had no effect on the CD44$^{-/-}$ AMΦ (**Figure 8c,d**), indicating that the interaction of HA on AMΦ promoted their survival. To determine whether this interaction also had similar consequences *in vivo*, KM81 was instilled into the lung on days 0, 2, 4, and 6 to disrupt the interaction. On day 7, AMΦ were isolated from the BAL, and the numbers of live, apoptotic, and dead cells were determined. KM81-treated mice had significantly more apoptotic and dead cells, and less live AMΦ cells than mice treated with an isotype-matched antibody (**Figure 8e–g**), demonstrating that the interaction of CD44 with HA on AMΦ in the alveolar space is required for their optimal survival and the maintenance of normal AMΦ numbers at homeostasis.

Figure 5 CD44 deficiency impairs the number of monocyte-derived alveolar macrophages (AMΦ) after lipopolysaccharide (LPS)-induced lung inflammation. (**a**) Schematic showing the intravenous (IV) transfer of 1–2 $\times$ 10^6 monocytes isolated from the bone marrow (BM) of CD45.2$^+$ CD44$^{+/+}$ and CD44$^{-/-}$ mice in a 1:1 ratio into host CD45.1$^+$ mice that were treated intratracheally (IT) with 25 µg of LPS 4 h earlier to induce acute lung inflammation. The bronchoalveolar lavage (BAL) was analyzed at days 14 and 30 after LPS treatment. (**b**) Representative flow cytometry plots showing the purity and proportion of CD44$^{+/+}$ and CD44$^{-/-}$ monocytes used for adoptive transfer. (**c**) Representative flow cytometry plots showing the proportion of CD44$^{+/+}$ and CD44$^{-/-}$ donor cells in the BAL at day 14 and comparing their phenotype. (**d**) Representative flow cytometry plots showing the proportion of CD44$^{+/+}$ and CD44$^{-/-}$ donor cells in the BAL at day 30 and comparing their phenotype. (**e**, **f**) Graphs comparing the percent of CD44$^{+/+}$ and CD44$^{-/-}$ donor cells in the BAL at days 14 and 30, respectively. Data show an average of two experiments ± s.d., each with three to five mice. Significance indicated as ***$P<0.001$, paired Student's *t*-test.

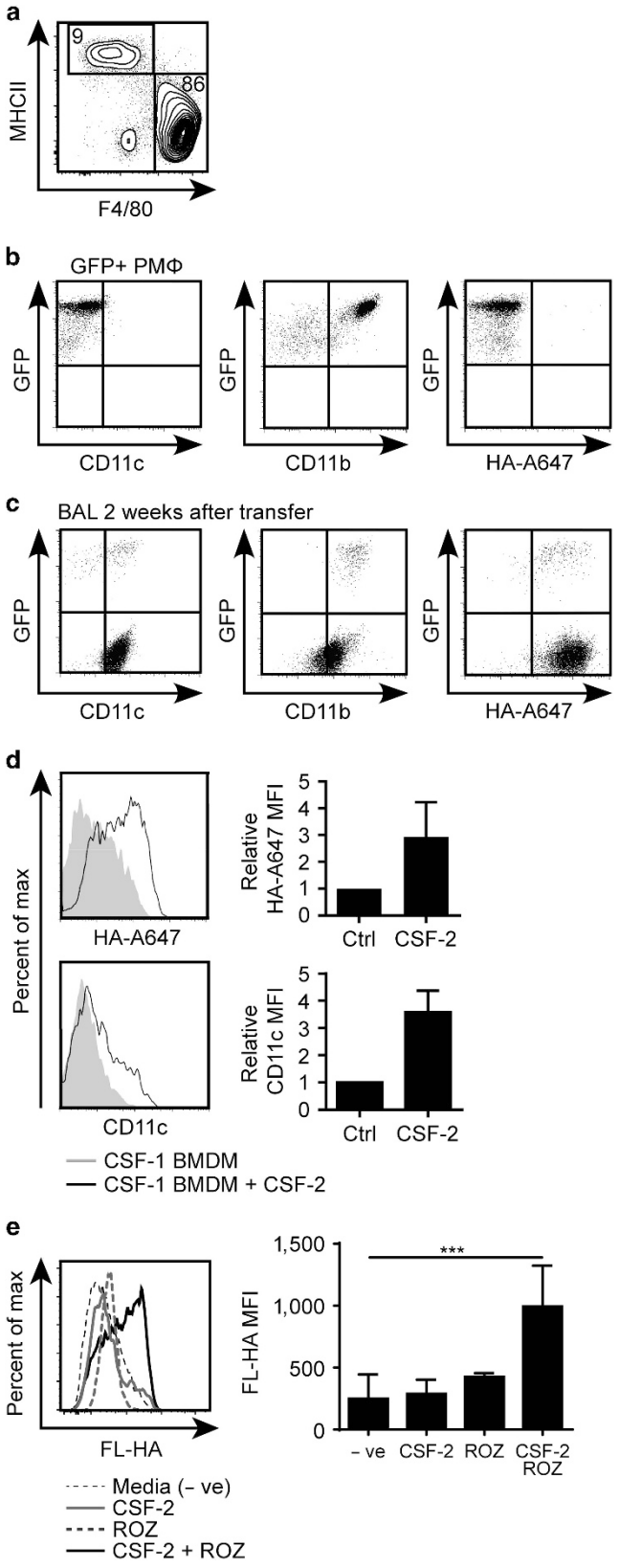

DISCUSSION

AMΦ develop from fetal monocytes and do not depend on adult monocytes for self-maintenance at homeostasis.[6,7] Here, we show that the self-renewal of AMΦ contributes to the rapid AMΦ repopulation 7 days after LPS-induced inflammation and AMΦ depletion. We also show that, in contrast to steady-state AMΦ maintenance, adult monocytes contribute to the AMΦ population after inflammation, although to a lesser extent and over a slower time frame of ~30 days. The relative contribution from AMΦ and monocytes may depend on the extent of lung damage and inflammation that, in turn, may affect the extent of AMΦ depletion. This initial depletion of AMΦ may alter the alveolar environment and expose a niche to allow monocyte engraftment and their subsequent differentiation into AMΦ. Although the transfer of GFP^+ monocytes provided evidence for their differentiation into cells with an AMΦ phenotype ($CD11c^+$, $CD11b^-$, Siglec F^+, HA binding, $SIRP\alpha^+$, $CD206^+$, $F4/80^{low}$) and similar proliferative capacity 45 days after lung inflammation, further transcriptomic and functional analysis is necessary before we can conclude that the monocytes have fully differentiated into *bona fide* AMΦ. Recent work shows monocyte-derived cells present in the lung 10 months after bleomycin-induced injury that express equal levels of Siglec F and have a very similar transcriptional signature to tissue-resident AMΦ.[26]

This report shows that the CD44 expressed on both fetal and BM-derived AMΦ is important for their survival. When $CD44^{+/+}$ and $CD44^{-/-}$ AMΦ were instilled into the lung, $CD44^{+/+}$ AMΦ outcompeted $CD44^{-/-}$ AMΦ under both noninflammatory and inflammatory conditions. In addition, BM-derived $CD44^{+/+}$ AMΦ were more prevalent than $CD44^{-/-}$ AMΦ after competitive BM reconstitution. This was a selective effect of CD44 on AMΦ, as donor-derived monocytes, neutrophils, and eosinophils all had equal proportions of $CD44^{+/+}$ and $CD44^{-/-}$ cells after BM reconstitution. Although all these cells express CD44, only AMΦ bind HA constitutively. Furthermore, when equal numbers of GFP^+ $CD44^{+/+}$ and $CD44^{-/-}$ BM-derived monocytes were adoptively transferred into the blood after LPS-induced lung inflammation, equal numbers of monocyte-derived cells were

Figure 6 The alveolar environment and colony-stimulating factor-2 (CSF-2) promote hyaluronan (HA) binding by macrophages. (**a**) Representative flow cytometry plot showing the expression of MHCII and F4/80 by purified peritoneal macrophages (PMΦ). (**b**) Representative flow cytometry plots showing the expression of CD11c, CD11b, and HA-A647 binding by GFP^+ PMΦ before or (**c**) 2 weeks after adoptive transfer intratracheally (IT) into the bronchoalveolar lavage (BAL). (**d**) Representative histograms of HA-A647 binding and CD11c expression of CSF-1-derived bone marrow-derived macrophages (BMDMs) treated with (black line) or without (shaded) CSF-2 for 48 h *in vitro*, and graphs of their relative mean fluorescent intensity (MFI). (**e**) Representative histogram and graph comparing fluorescein-conjugated HA (FL-HA) binding by PMΦ treated for 7 days *in vitro* with CSF-2 alone, rosiglitazone (ROZ) alone, or CSF-2 and ROZ. **a** and **b** are representative plots of six mice examined over two experiments. Graphs show an average of two experiments ± s.d., each with three to five mice. Significance indicated as $***P<0.001$, paired Student's *t*-test.

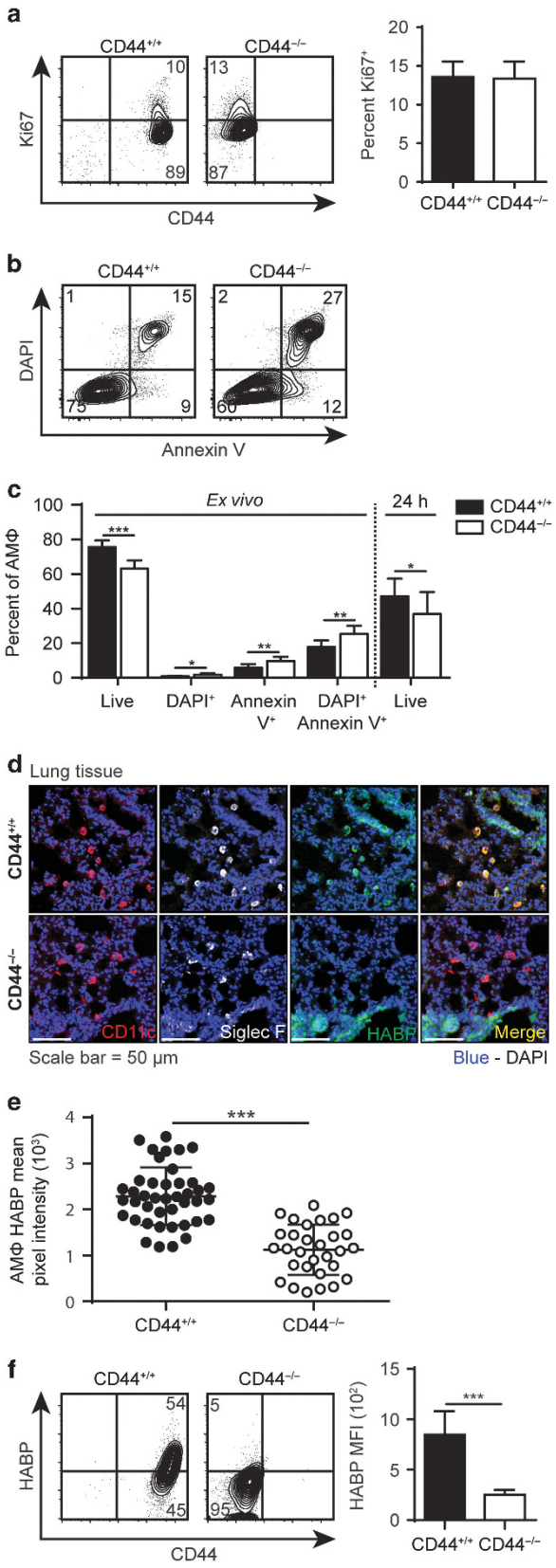

present at day 14. It was only by day 30, when they had gained the full HA binding AMΦ phenotype, that the CD44$^{+/+}$ AMΦ had an advantage. Together, this shows that CD44 exerts its competitive advantage on AMΦ, not monocytes, correlating with its ability to bind HA.

Previous studies have shown that instillation of PMΦ into the alveolar environment changes their transcriptional signature and phenotype toward that of an AMΦ,[8] although CD11b remains high. Another study also showed phenotypic changes when PMΦ were instilled into the alveolar space of Csf2rb$^{-/-}$ mice.[9] However, in both studies, very few cells repopulated the alveolar space, and after 8 weeks these cells did not rescue alveolar proteinosis in the Csf2rb$^{-/-}$ mice, whereas monocytes did.[9] Here, we found that HA binding, a key characteristic of AMΦ, was induced on PMΦ by the alveolar environment after 2 weeks, but CD11b remained high. As this PMΦ instillation contained a majority of tissue-resident PMΦ and a minority of F4/80^{low} macrophages, we cannot precisely determine the origin of these cells. However, HA binding was induced when these PMΦ were exposed to both CSF-2 and the PPARγ agonist, ROZ, *in vitro*, suggesting that these two signals may be responsible for the induction of HA binding by macrophages in the alveolar space. CSF-2 induces the expression of the nuclear receptor PPARγ,[5] and both are required for the differentiation of fetal monocytes into AMΦ *in vivo*.[4,6] The induction of constitutive HA binding by the alveolar environment is a striking feature, as monocytes and PMΦ do not normally bind detectable levels of exogenously added HA, unless they are exposed to inflammatory stimuli.[24,27,28] However, AMΦ are not unique in their constitutive ability to engage HA, as splenic F4/80^{+} macrophages can also bind HA,[29] and PMΦ are recruited to the site of liver injury in a CD44- and HA-dependent manner.[30] Together, these highlight the importance of environmental imprinting on HA binding and macrophage phenotype.

Figure 7 CD44$^{-/-}$ alveolar macrophages (AMΦ) have increased cell death and do not bind hyaluronan (HA) on the cell surface. (**a**) Representative flow cytometry plots and graph comparing Ki67 expression on *ex vivo* CD44$^{+/+}$ and CD44$^{-/-}$ AMΦ. (**b**) Representative flow cytometry plots comparing *ex vivo* CD44$^{+/+}$ and CD44$^{-/-}$ AMΦ survival by 4',6-diamidino-2-phenylindole (DAPI) and Annexin V labeling. (**c**) Percent of CD44$^{+/+}$ and CD44$^{-/-}$ AMΦ that are alive, apoptotic (Annexin V^{+}), or dead (DAPI^{+} or Annexin V^{+}, DAPI^{+}) from *ex vivo* cells and percent live cells after 24 h in culture. (**d**) Confocal microscopy of CD44$^{+/+}$ and CD44$^{-/-}$ lung tissue labeled with DAPI (blue), CD11c (red), Siglec F (white), and HABP (green); merged (yellow) image is of CD11c and HA binding protein (HABP). Image is representative of six mice over two experiments. (**e**) Comparing mean pixel intensity of labeled HABP from confocal microscopy of CD44$^{+/+}$ and CD44$^{-/-}$ AMΦ in the lung tissue. Individual cell measurements were from 3 mice, 2 fields each, and the average ± s.d. with ***$P<0.001$, nonparametric unpaired Mann–Whitney test. (**f**) Flow cytometry of CD44 and the binding of biotinylated HABP to the surface of *ex vivo* CD44$^{+/+}$ and CD44$^{-/-}$ AMΦ detected by streptavidin-PE-Cy7 and the graph showing the average mean fluorescent intensity (MFI) of HABP binding from 6 mice. Graphs in **a**, **c**, and **f** show the average from two experiments ± s.d., each with cells from three to five mice. Significance indicated as *$P<0.05$, **$P<0.01$, ***$P<0.001$ nonpaired Student's *t*-test.

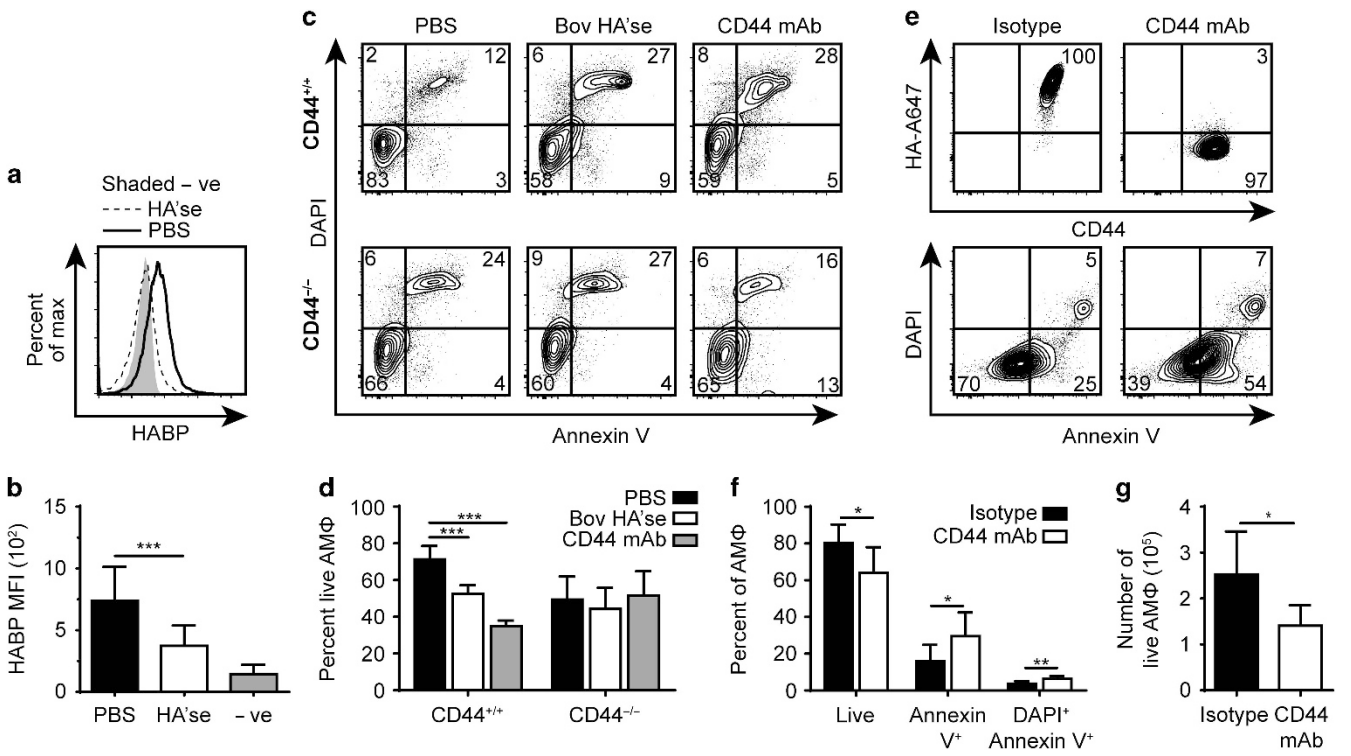

Figure 8 Hyaluronan (HA) binding to CD44 promotes alveolar macrophage (AMΦ) survival. (**a**, **b**) Histogram and graph showing the mean fluorescent intensity (MFI) of HA binding protein (HABP) labeling of surface HA on *ex vivo* AMΦ before and after bovine hyaluronidase (Bov HA'se) treatment. (**c**) Representative flow cytometry plots of $CD44^{+/+}$ or $CD44^{-/-}$ AMΦ labeled with 4',6-diamidino-2-phenylindole (DAPI) and Annexin V after PBS, Bov HA'se, or CD44 monoclonal antibody (mAb) (KM81) treatment for 1 h, and (**d**) percent live $CD44^{+/+}$ or $CD44^{-/-}$ AMΦ (Annexin V^- $DAPI^-$) after treatment. (**e**) Representative flow cytometry plots of bronchoalveolar lavage (BAL) cells from mice after treatment with isotype-matched or CD44 mAb delivered intratracheally (IT) on days 0, 2, 4, and 6, then isolated on day 7 and labeled with CD44, HA-A647, DAPI, and Annexin V. (**f**) Percent AMΦ in the BAL that are alive, apoptotic (Annexin V^+), or dead ($DAPI^+$ or Annexin V^+) after 7 days of isotype or CD44 mAb antibody treatment. (**g**) Number of live AMΦ in the BAL after 7 days of isotype or CD44 mAb antibody treatment. Data show an average of two experiments ± s.d., each with three to five mice. Significance indicated as $^*P<0.05$, $^{**}P<0.01$, $^{***}P<0.001$, paired (**b**, **d**) and nonpaired (**f**, **g**) Student's *t*-test.

Results from *in vivo* competition in wild-type mice show that CD44-deficient AMΦ have an intrinsic defect that may be because of their inability to bind HA. The presence of cell surface HA is a major difference between $CD44^{+/+}$ and $CD44^{-/-}$ AMΦ. $CD44^{+/+}$, but not $CD44^{-/-}$, AMΦ are decorated with HA *in vivo*. This was somewhat unexpected as others have shown that alveolar macrophages readily take up and degrade HA *in vitro* and *in vivo* during lung development.[17,18] Nevertheless, surface-bound HA was functionally important as prevention of HA binding by a CD44 blocking antibody both *ex vivo* and *in vivo* or by enzymatic removal of HA on *ex vivo* cells reduced the survival of $CD44^{+/+}$ AMΦ. Thus, we conclude the interaction of CD44 with HA provides a survival advantage for AMΦ. Supporting this, $CD44^{-/-}$ mice had decreased numbers of AMΦ in the alveolar space, and $CD44^{-/-}$ AMΦ were more susceptible to cell death. Together, this demonstrates the importance of the HA coat and its interaction with CD44 in AMΦ survival.

In the alveolar space, AMΦ reside between the surfactant and the alveolar epithelial cells (AECs).[3] Thus, one possible source of HA in the alveolar space is AECs. Type II AECs (AEC2) express hyaluronan synthase 2 and display HA on their surface[31] that may promote interactions with AMΦ. Other molecular interactions already exist between AECs and AMΦ that provide inhibitory signals to prevent AMΦ activation.[3] AMΦ binding to AECs may also facilitate AMΦ proximity to AEC-derived growth and survival factors such as CSF-2, to help sustain lung homeostasis.[32] Alternatively, HA may be scavenged from these cells and from the alveolar space, or AMΦ themselves may synthesize HA that is then bound by surface CD44. Extracellular HA binding by CD44 on AMΦ could be integral to forming a HA-rich glycocalyx that may promote cell survival by protecting against environmental stress, for example, by protecting against reactive oxygen species,[33,34] or against sheer stress.[35] Alternatively, HA binding to CD44 on AMΦ may provide prosurvival signals. High expression of CD44 has been linked with promoting effector T-cell survival and protection from Fas-mediated apoptosis in T helper type 1 cells[36] and antibody-induced CD44 ligation improves survival and resistance of cancer cells to drug-induced apoptosis.[37–39] However, it has been difficult to identify HA-mediated signaling events in cells.[40]

AEC2 have stem cell-like properties in the adult lung and contribute to tissue repair. In a mouse model of bleomycin-induced lung damage, AEC2 cells lacking HAS2 had lower levels of surface HA, showed increased apoptosis, and a reduced ability to proliferate and form colonies, implicating a role for surface HA in the survival and proliferation of AEC2.[31]

Furthermore, AEC2 from idiopathic pulmonary fibrosis patients also showed reduced surface HA and were less efficient in generating colonies compared with AEC2 from healthy individuals.[31] Similarly, CD44 and its interactions with HA have been implicated in promoting the self-renewal and survival of cancer-initiating cells.[41] Here, we add to this accumulating evidence for a role of HA binding by CD44 in promoting the survival of cells with stem cell-like renewal capacity by showing that HA–CD44 interactions support the survival of long-lived, self-renewing AMΦ. The specific effect of HA binding by CD44 on AMΦ survival highlights both CD44 and HA as possible targets for therapeutic intervention. Given the importance of AMΦ in maintaining lung immunosurveillance and homeostasis, strategies that improve the survival or self-renewal potential of these cells, especially in pathological conditions of lung inflammation, may result in therapeutic benefits.

METHODS

Mice. C57BL/6J (CD45.2$^+$) and B6.SJL-*Ptprc*^{a}*Pepc*^{b}/BoyJ (CD45.1$^+$) mice were from Jackson Laboratory (Bar Harbor, ME). These mice, and CD44$^{-/-}$ mice[42] backcrossed with C57BL/6J mice for 9 generations, were housed and bred at the University of British Columbia (UBC, Vancouver, BC, Canada). Mating C57BL/6J and BoyJ mice gave C57BL/6JxBoyJ heterozygotes (CD45.1$^+$, CD45.2$^+$). C57BL/6 mice expressing GFP from an α-actin-CMV hybrid promoter were provided by Dr Fabio Rossi (UBC) and cells from heterozygous GFP$^+$ mice were used for the adoptive transfer experiments. All animal experiments were conducted with protocols approved by the University Animal Care Committee in accordance with the Canadian Council of Animal Care guidelines for ethical animal research.

Reagents. L-cell conditioned media containing CSF-1 were generated from L929 fibroblast cells and tissue culture supernatant from J558L cells was the source of CSF-2, as described previously.[16,29] Fluorescein-conjugated HA was prepared using hyaluronic acid sodium salt from Rooster comb (Sigma-Aldrich, St. Louis, MO), as described previously.[43] High-molecular-weight HA (Lifecore Biomedical, Chaska, MN) was conjugated with Alexa Fluor-647 by AbLab (UBC) for HA-A647. Purified low endotoxin, HA-blocking, rat anti-mouse CD44 mAb, KM81, and rat IgG2a isotype-matched mAb were purchased from Cedarlane Laboratories (Burlington, ON, Canada). Recombinant mouse CSF-2 (carrier free) was purchased from BioLegend (San Diego, CA). Rosiglitazone (ROZ) was purchased from Cayman Chemical Company (Ann Harbor, MI).

Flow cytometry (FC). Cells were incubated with 2.4G2 tissue culture supernatant for 20 min to block Fc receptors, washed with FC buffer (PBS, 2% bovine serum albumin, and 2 mM EDTA), labeled with mAbs and/or fluorescein-conjugated HA for 20 min at 4 °C, washed twice in FC buffer, and resuspended in FC buffer containing propidium iodide, DAPI, or Live/Dead Fixable Aqua Dead Cell Stain (ThermoFisher, Waltham, MA) to label nonviable cells. For intracellular labeling, cells were fixed in 4% paraformaldehyde for 10 min at room temperature, permeabilized with PBS, 2 mM EDTA, 0.1% saponin, 1% bovine serum albumin for 30 min at room temperature, and then incubated with intracellular mAb. The following mAbs against mouse antigens were used for flow cytometry, cell isolation, or confocal imaging: CD11c (N418), F4/80 (BM8), CD44 (IM7), CD11b (M1/70), MHCII (M5/114.15.2), CD45.1 (A20), CD45.2 (104), CD206 (C068C2), Ki67 (SolA15), Ly6C (HK1.4), Ly6G (1A8), Siglec F (E50-2440 or 1RNM44N), and SIRPα (P84). Antibodies were purchased from Affymetrix eBioscience (Waltham, MA, USA), R&D Systems (Minneapolis, MN), BD Biosciences (San Jose, CA), or AbLab (UBC). Cells were processed on an LSR II (BD Biosciences) or MACSQuant (Miltenyi Biotec, Auburn, CA) flow cytometer.

Cell isolation. Mice were killed by isoflurane overdose. BAL cells were harvested by catheterization of the trachea and washing thrice with 1 ml FC buffer. BAL cells were centrifuged and resuspended in red blood cell lysis buffer (0.84% NH_4Cl in 10 mM Tris buffer, pH 7.2) for 5 min, and then centrifuged again and resuspended in FC buffer. The whole lung was then perfused with PBS via cardiac puncture of the right ventricle and harvested, minced, incubated in RPMI (with 0.7 mg ml^{-1} Collagenase IV (Worthington, Lakewood, NJ), 50 μg ml^{-1} of DNAse I (Worthington) for 1 h at 37 °C, and passed through a 70 μm cell strainer to generate the lung single-cell suspension that was treated with red blood cell lysis buffer, passed through a 35 μm cell strainer, and resuspended in FC buffer.

The peritoneal lavage, obtained with 5 ml of PBS, was centrifuged and treated with red blood cell lysis buffer for 5 min, then centrifuged and resuspended in FC buffer, incubated with 2.4G2 for 20 min, and labeled with biotinylated F4/80 antibody for 20 min. Then, PMΦ were isolated with anti-biotin MicroBeads and LS columns (Miltenyi Biotec) according to the manufacturer's instructions. Purity was 85% or above for the F4/80^{high} macrophages. Monocytes were isolated from the BM using the EasySep Mouse Monocyte Isolation Kit (Stemcell Technologies, Vancouver, BC, Canada) according to the manufacturer's instructions, and their purity was assessed by FC.

Induction of lung inflammation and adoptive monocyte transfer. Mice were treated with 25 μg of *Escherichia coli* 0111:B4 LPS (Sigma-Aldrich) in 50 μl PBS via IT instillation. After 4 h, 0.5–1 × 10^6 GFP$^+$ BM monocytes resuspended in 200 μl PBS were injected IV into C57BL/6J host mice. Alternatively, 1–2 × 10^6 CD45.2$^+$ CD44$^{+/+}$ and CD44$^{-/-}$ monocytes (1:1 ratio) were injected IV into the LPS-treated CD45.1 host. The lung and BAL were harvested at indicated times following LPS for FC analysis. The weight of LPS-treated mice were recorded daily for 7 days, and then on days 14 and 30.

Competitive BM reconstitution. 8 × 10^6 CD45.1$^+$ CD45.2$^+$ CD44$^{+/+}$ and CD45.2$^+$ CD44$^{-/-}$ BM cells (1:1 ratio) were injected IV into lethally irradiated (24 h after gamma radiation 6.5 Gy, twice, 4 h apart) CD45.1$^+$ host mice. The perfused lung and BAL were harvested after 7 weeks for analysis.

Intratracheal instillation of AMΦ and PMΦ. GFP$^+$ AMΦ (3 × 10^5) in 50 μl PBS were instilled IT into CD45.2$^+$ mice. BAL was collected at the indicated time points for analysis. Alternatively, 3 × 10^5 CD45.2$^+$ CD44$^{+/+}$ and CD44$^{-/-}$ AMΦ (1:1 ratio) in 50 μl PBS were instilled IT into CD45.1$^+$ mice. Some mice were challenged with 25 μg of LPS 24 h following the instillation of donor AMΦ. The BAL was collected 24 h or 8 days after AMΦ instillation for analysis.

PMΦ were isolated from GFP$^+$ mice as described above. CD45.1$^+$ or CD45.1$^+$ CD45.2$^+$ mice received 8 × 10^5 GFP$^+$ PMΦ in 50 μl PBS by IT instillation. The BAL was collected 2 weeks later for analysis.

Intratracheal instillation of HA blocking CD44 antibody. Four separate doses of 50 μg of the HA blocking CD44 mAb, KM81, or an isotype-matched rat IgG2a mAb were instilled IT into isoflurane-anesthetized CD45.2$^+$ mice on days 0, 2, 4, and 6. The BAL was collected on day 7 for FC analysis.

AMΦ Ki67 labeling. AMΦ were treated with 2.4G2 to block Fc receptors, labeled with CD44 antibody, and incubated with LIVE/DEAD Fixable Aqua Dead Cell Stain for 30 min. Cells were then fixed and permeabilized, incubated with 2.4G2, and labeled with fluorescent Ki67 antibody for FC analysis.

Generation of CSF-1 derived BMDMs. BM was isolated from murine femurs and tibia, and CSF-1-derived BMDMs were generated as previously described.[29]

Macrophage stimulation with CSF-2 and ROZ. CSF-1 BMDMs (2×10^5) were collected on day 5 and cultured in 200 µl Dulbecco's modified Eagle's medium DMEM (Invitrogen, Carlsbad, CA) with 10% fetal calf serum in nontissue culture-treated 96-well plates in the presence or absence of 4% CSF-2 containing supernatant for 48 h. Cells were then analyzed by FC. Purified F4/80$^+$ PMΦ (2×10^5) were cultured in 200 µl complete RPMI-1640 media (with 10% fetal calf serum, 20 mM HEPES, 1 × nonessential amino acid, 55 µM 2-mercaptoethanol, 1 mM sodium pyruvate, 2 mM L-glutamine, 50 U ml^{-1} penicillin/streptomycin, all from Invitrogen) in nontissue culture-treated 96-well plates in the presence or absence of 20 ng ml^{-1} of mouse recombinant CSF-2, 1 µM ROZ, or 20 ng ml^{-1} of CSF-2 and 1 µM ROZ for 7 days, with a media change at days 3 and 6. Cells were analyzed by FC on day 7.

Measuring AMΦ cell death and surface HA labeling. AMΦ were labeled with DAPI and fluorescent Annexin V in 10 mM HEPES (pH 7.4), 140 mM NaCl, and 2.5 mM $CaCl_2$ for 20 min for FC analysis. Alternatively, 1×10^5 cells were plated in 96-well nontissue culture-treated plates in complete RPMI-1640 media and incubated at 37 °C. After 24 h, the cells were collected with Versene and analyzed for Annexin V and DAPI. Cell surface HA for FC was determined by biotinylated HABP (Millipore Sigma, St. Louis, MO) and streptavidin-PE-Cy7 (Affymetrix eBioscience) labeling. AMΦ were incubated in 100 µl PBS containing 20 U of bovine hyaluronidase (Sigma-Aldrich) or 100 µl of KM81 hybridoma (ATCC, Manassas, VA, TIB-241) tissue culture supernatant containing the CD44 blocking antibody KM81 for 1 h at 37 °C to remove surface HA or block CD44–HA interactions, respectively.

Confocal microscopy. Lungs were harvested from isoflurane-anesthetized mice and fixed by immersing into ice-cold 4% paraformaldehyde for 2 h. Fixed tissue was embedded in NEG-50 freezing matrix (ThermoFisher) and snap frozen in dry ice cooled isopentane. Then, 12 µm cryosections were cut and thaw mounted onto Superfrost Plus microscope slides (ThermoFisher). Tissue sections were fixed again with acetone, blocked with 10% goat serum, and labeled with CD11c and Siglec F antibodies followed by goat-anti hamster Alexa 647 and goat anti-rat Alexa 488 (ThermoFisher) respectively and biotinylated HABP followed by streptavidin Alexa 568 (ThermoFisher). Images were acquired using the 20 × dry objective of a FV1000 laser scanning confocal microscope (Olympus, Richmond Hill, ON, Canada) equipped with 405, 488, 543, and 633 nm laser lines.

Data analysis. FC was analyzed using FlowJo VX (Treestar, Ashland, OR). Flow cytometry plots shown were first gated by size, singlets, and live/dead stain. Graphs were generated using GraphPad Prism 6 (La Jolla, CA). Data shown are the average ± s.d. Significance was determined by Student's two-tailed, unpaired or paired *t*-test with $^*P<0.05$, $^{**}P<0.01$, and $^{***}P<0.001$. Confocal microscopy was analyzed using the Fiji distribution package of ImageJ 1.51 (NIH, Rockville, MD). The mean pixel intensity of HABP for CD11c$^+$ Siglec F$^+$ CD44$^{+/+}$ or CD44$^{-/-}$ AMΦ was determined, data shown are individual cell measurements and the average ± s.d., and statistical significance was tested by nonparametric unpaired Mann–Whitney test with $^{***}P<0.001$.

ACKNOWLEDGMENTS

This work was supported by grants from the Natural Sciences and Engineering Council of Canada (NSERC) and the Canadian Institutes of Health Research (MOP 119503) to P.J. A.A.A, Y.D., and S.M.L.-S. acknowledge fellowships from NSERC and UBC. We also acknowledge invaluable assistance from the UBC Animal and Flow Cytometry Facilities.

AUTHOR CONTRIBUTIONS

G.F.T.P., Y.D., and P.J. developed the project; Y.D. performed most of the experiments and analyzed the data, followed by G.F.T.P. and then A.A.A. and S.M.L.-S. M.D. provided technical support. Y.D. and P.J. wrote the manuscript that was reviewed and edited by all authors.

DISCLOSURE

The authors declared no conflict of interest.

REFERENCES

1. Iwasaki, A., Foxman, E.F. & Molony, R.D. Early local immune defences in the respiratory tract. *Nat. Rev. Immunol.* **17**, 7–20 (2017).
2. Kopf, M., Schneider, C. & Nobs, S.P. The development and function of lung-resident macrophages and dendritic cells. *Nat. Immunol.* **16**, 36–44 (2014).
3. Hussell, T. & Bell, T.J. Alveolar macrophages: plasticity in a tissue-specific context. *Nat. Rev. Immunol.* **14**, 81–93 (2014).
4. Shibata, Y., Berclaz, P.Y., Chroneos, Z.C., Yoshida, M., Whitsett, J.A. & Trapnell, B.C. GM-CSF regulates alveolar macrophage differentiation and innate immunity in the lung through PU.1. *Immunity* **15**, 557–567 (2001).
5. Schneider, C., Nobs, S.P., Kurrer, M., Rehrauer, H., Thiele, C. & Kopf, M. Induction of the nuclear receptor PPAR-gamma by the cytokine GM-CSF is critical for the differentiation of fetal monocytes into alveolar macrophages. *Nat. Immunol.* **15**, 1026–1037 (2014).
6. Guilliams, M. *et al.* Alveolar macrophages develop from fetal monocytes that differentiate into long-lived cells in the first week of life via GM-CSF. *J. Exp. Med.* **210**, 1977–1992 (2013).
7. Hashimoto, D. *et al.* Tissue-resident macrophages self-maintain locally throughout adult life with minimal contribution from circulating monocytes. *Immunity* **38**, 792–804 (2013).
8. Lavin, Y. *et al.* Tissue-resident macrophage enhancer landscapes are shaped by the local microenvironment. *Cell* **159**, 1312–1326 (2014).
9. van de Laar, L. *et al.* Yolk sac macrophages, fetal liver, and adult monocytes can colonize an empty niche and develop into functional tissue-resident macrophages. *Immunity* **44**, 755–768 (2016).
10. Guilliams, M. & Scott, C.L. Does niche competition determine the origin of tissue-resident macrophages?. *Nat. Rev. Immunol.* **17**, 451–460 (2017).
11. Maus, U.A. *et al.* Resident alveolar macrophages are replaced by recruited monocytes in response to endotoxin-induced lung inflammation. *Am. J. Respir. Cell Mol. Biol.* **35**, 227–235 (2006).
12. Dockrell, D.H. *et al.* Alveolar macrophage apoptosis contributes to pneumococcal clearance in a resolving model of pulmonary infection. *J. Immunol.* **171**, 5380–5388 (2003).
13. Pribul, P.K. *et al.* Alveolar macrophages are a major determinant of early responses to viral lung infection but do not influence subsequent disease development. *J. Virol.* **82**, 4441–4448 (2008).
14. Thepen, T., Van Rooijen, N. & Kraal, G. Alveolar macrophage elimination in vivo is associated with an increase in pulmonary immune response in mice. *J. Exp. Med.* **170**, 499–509 (1989).
15. Knapp, S. *et al.* Alveolar macrophages have a protective antiinflammatory role during murine pneumococcal pneumonia. *Am. J. Respir. Crit. Care Med.* **167**, 171–179 (2003).
16. Poon, G.F. *et al.* Hyaluronan binding identifies a functionally distinct alveolar macrophage-like population in bone marrow-derived dendritic cell cultures. *J. Immunol.* **195**, 632–642 (2015).
17. Culty, M., O'Mara, T.E., Underhill, C.B., Yeager, H. Jr. & Swartz, R.P. Hyaluronan receptor (CD44) expression and function in human peripheral blood monocytes and alveolar macrophages. *J. Leukoc. Biol.* **56**, 605–611 (1994).
18. Underhill, C.B., Nguyen, H.A., Shizari, M. & Culty, M. CD44 positive macrophages take up hyaluronan during lung development. *Dev. Biol.* **155**, 324–336 (1993).
19. Teder, P. *et al.* Resolution of lung inflammation by CD44. *Science* **296**, 155–158 (2002).
20. Liang, J.R. *et al.* CD44 is a negative regulator of acute pulmonary inflammation and lipopolysaccharide-TLR signaling in mouse macrophages. *J. Immunol.* **178**, 2469–2475 (2007).
21. McDonald, B. & Kubes, P. Interactions between CD44 and hyaluronan in leukocyte trafficking. *Front. Immunol.* **6**, 68 (2015).
22. Guth, A.M. *et al.* Lung environment determines unique phenotype of alveolar macrophages. *Am. J. Physiol. Lung Cell. Mol. Physiol.* **296**, L936–L946 (2009).

23. Bain, C.C. *et al.* Long-lived self-renewing bone marrow-derived macrophages displace embryo-derived cells to inhabit adult serous cavities. *Nat. Commun.* **7**, ncomms11852 (2016).
24. Ruffell, B. *et al.* Differential use of chondroitin sulfate to regulate hyaluronan binding by receptor CD44 in inflammatory and Interleukin 4-activated macrophages. *J. Biol. Chem.* **286**, 19179–19190 (2011).
25. Camp, H.S. *et al.* Differential activation of peroxisome proliferator-activated receptor-gamma by troglitazone and rosiglitazone. *Diabetes* **49**, 539–547 (2000).
26. Misharin, A.V. *et al.* Monocyte-derived alveolar macrophages drive lung fibrosis and persist in the lung over the life span. *J. Exp. Med.* **214**, 2387–2404 (2017).
27. Levesque, M.C. & Haynes, B.F. Cytokine induction of the ability of human monocyte CD44 to bind hyaluronan is mediated primarily by TNF-alpha and is inhibited by IL-4 and IL-13. *J. Immunol.* **159**, 6184–6194 (1997).
28. Brown, K.L., Maiti, A. & Johnson, P. Role of sulfation in CD44-mediated hyaluronan binding induced by inflammatory mediators in human CD14 + peripheral blood monocytes. *J. Immunol.* **167**, 5367–5374 (2001).
29. Dong, Y.F. *et al.* Endotoxin free hyaluronan and hyaluronan fragments do not stimulate TNF-alpha, interleukin-12 or upregulate co-stimulatory molecules in dendritic cells or macrophages. *Sci. Rep.* **6**, 36928 (2016).
30. Wang, J. & Kubes, P. A reservoir of mature cavity macrophages that can rapidly invade visceral organs to affect tissue repair. *Cell* **165**, 668–678 (2016).
31. Liang, J. *et al.* Hyaluronan and TLR4 promote surfactant-protein-C-positive alveolar progenitor cell renewal and prevent severe pulmonary fibrosis in mice. *Nat. Med.* **22**, 1285–1293 (2016).
32. Huffman, J.A., Hull, W.M., Dranoff, G., Mulligan, R.C. & Whitsett, J.A. Pulmonary epithelial cell expression of GM-CSF corrects the alveolar proteinosis in GM-CSF-deficient mice. *J. Clin. Invest.* **97**, 649–655 (1996).
33. Sato, H. *et al.* Antioxidant activity of synovial fluid, hyaluronic acid, and two subcomponents of hyaluronic acid. Synovial fluid scavenging effect is enhanced in rheumatoid arthritis patients. *Arthritis Rheum.* **31**, 63–71 (1988).
34. Presti, D. & Scott, J.E. Hyaluronan-mediated protective effect against cell-damage caused by enzymatically produced hydroxyl (OH.) radicals is dependent on hyaluronan molecular-mass. *Cell Biochem. Funct.* **12**, 281–288 (1994).
35. Gouverneur, M., Spaan, J.A.E., Pannekoek, H., Fontijn, R.D. & Vink, H. Fluid shear stress stimulates incorporation of hyaluronan into endothelial cell glycocalyx. *Am. J. Physiol. Heart Circ. Physiol.* **290**, H458–H462 (2006).
36. Baaten, B.J.G., Li, C.R., Deiro, M.F., Lin, M.M., Linton, P.J. & Bradley, L.M. CD44 regulates survival and memory development in Th1 Cells. *Immunity* **32**, 104–115 (2010).
37. Herishanu, Y. *et al.* Activation of CD44, a receptor for extracellular matrix components, protects chronic lymphocytic leukemia cells from spontaneous and drug induced apoptosis through MCL-1. *Leuk. Lymphoma* **52**, 1758–1769 (2011).
38. Bates, R.C., Edwards, N.S., Burns, G.F. & Fisher, D.E. A CD44 survival pathway triggers chemoresistance via lyn kinase and phosphoinositide 3-kinase/Akt in colon carcinoma cells. *Cancer Res.* **61**, 5275–5283 (2001).
39. Allouche, M., Charrad, R.S., Bettaieb, A., Greenland, C., Grignon, C. & Smadja-Joffe, F. Ligation of the CD44 adhesion molecule inhibits drug-induced apoptosis in human myeloid leukemia cells. *Blood* **96**, 1187–1190 (2000).
40. Lee-Sayer, S.S.M., Dong, Y., Arif, A.A., Olsson, M., Brown, K.L. & Johnson, P. The where, when, how, and why of hyaluronan binding by immune cells. *Front. Immunol.* **6**, 150 (2015).
41. Chanmee, T., Ontong, P., Kimata, K. & Itano, N. Key roles of hyaluronan and its CD44 receptor in the stemness and survival of cancer stem cells. *Front. Oncol.* **5**, 180 (2015).
42. Schmits, R. *et al.* CD44 regulates hematopoietic progenitor distribution, granuloma formation, and tumorigenicity. *Blood* **90**, 2217–2233 (1997).
43. de Belder, A.N. & Wik, K.O. Preparation and properties of fluorescein-labelled hyaluronate. *Carbohydr. Res.* **44**, 251–257 (1975).